Optimization of Base Thermal Protection System for Advanced Saturn II Boosters Employing Strap-On Solid-Propellant Motors

M. B. HAMMOND,* B. K. ADLER,† AND K. D. KORKAN‡
North American Rockwell Corp., Downey, Calif.

The potential application of the Saturn II employing four solid-rocket motors (SRM's) as a first-stage booster has been studied to provide intermediate payload capability between the Saturn I and Saturn V. The result of the selection of four 120-in. solid-rocket motors has been an increase in the heating environment in the base area requiring redesign of the current base-area thermal protection. Base thermal environment analyses indicate that heating is mainly from plume radiation from the SRM's for the first 70 sec after lift-off. After J-2 liquid H_2-O_2 engine ignition at 70 sec, a convective recirculating heat flux is superimposed on the radiative heating until SRM separation. The base thermal protection system studied consists of 1) a complete base close-out shield over the aft end of the S-II stage which maintains the J-2 engines at −150°F prior to ignition, and 2) a modified version of the current base heat shield to protect the base-area equipment and structure. The thermal protection systems examined in detail include a heat-reflecting ceramic material (identified as M-31) and an ablative phenolic-impregnated cork insulation. It is concluded that the full base close-out should be designed to incorporate the heat-reflecting ceramic material, and that the inner heat shield should employ an ablative cork material applied to the current S-II heat shield.

Nomenclature

C	=	specific heat
H	=	heat of ablation
h	=	convective heat-transfer coefficient
i	=	enthalpy
k	=	thermal conductivity
q	=	heat-transfer rate
T	=	temperature
t	=	time
U	=	velocity of "charring" surface
V	=	$T - T_0$
W	=	weight per unit area
x	=	distance into thermal protection from surface
α	=	absorptivity
ϵ	=	emissivity
ρ	=	density

Subscripts

char	=	char material
conv	=	convection
in	=	into surface
0, r, w	=	initial, recovery, and wall, respectively
rad	=	heat radiated from surface

Introduction

STUDIES of modified Saturn V launch vehicles were initiated by Marshall Space Flight Center in late 1965 in order to bridge the payload capability gap between the Saturn I and Saturn V.[1] In this study, the North American Aviation Space Division was assigned the prime responsibility of examining the possible application of the S-II stage in combination with SRM's to provide first-stage performance. The S-II is powered by five J-2 rocket engines using liquid hydrogen (LH_2) and oxygen (LOX) and having a vacuum thrust of one million lb. One of the systems resulting from this study was a design employing four strap-on United Technology Center (UTC) 1207, 120-in., seven-segment SRM's as shown in Fig. 1, having a sea-level thrust of 4×10^6 lb. Studies of optimum staging indicated that the J-2 engines should be ignited at 70 sec of boost following lift-off with separation of the SRM's at approximately 120 sec. The high radiant heating from the SRM boosters makes it necessary to provide a full base close-out heat shield over the aft end of the S-II for the first 70 sec to maintain the proper thermal environment for J-2 engine ignition. The combined radiant and convective heating factors existing between J-2 ignition and SRM tailoff required a modification of the current S-II base thermal protection, which was designed for high-altitude J-2 engine operation only. The results of analyses to optimize the base thermal protection system for the advanced S-II with strap-on SRM boosters are provided in this paper.

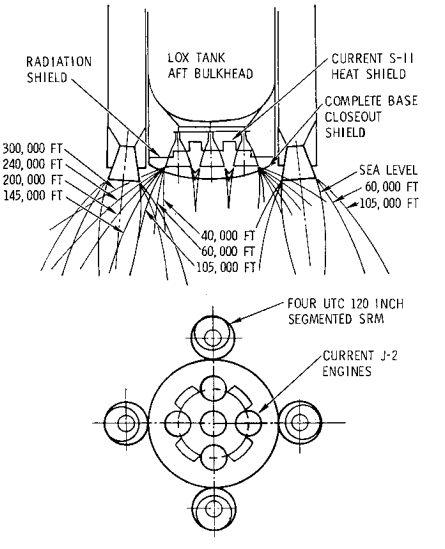

Fig. 1 Base configuration of study vehicle and associated plume boundaries.

Presented at the AIAA/ASME 8th Structures, Structural Dynamics and Materials Conference, Palm Springs, Calif., March 29–31, 1967 (no paper number; published in bound volume of conference papers); submitted April 21, 1967; revision received August 7, 1967. Work conducted under NASA Marshall Space Flight Center Contract NAS8-20265. [6.08, 6.12, 11.20]

* Senior Technical Specialist, Space Division. Member AIAA.
† Research Engineer, Space Division. Member AIAA.
‡ Senior Research Engineer, Space Division. Member AIAA.

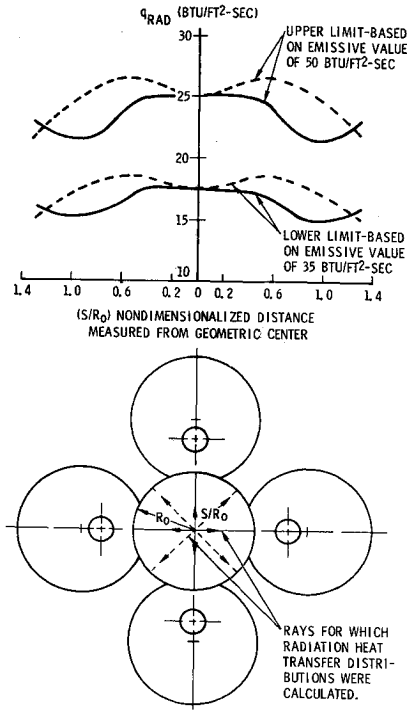

Fig. 2 Solid-particle radiation heat-transfer distributions on full base close-out.

Base Thermal Environment

The heating rates and related pressures in the base area of the S-II stage are altitude functions of the plume characteristics and the associated flow phenomena. The methods outlined by Etemad and Korkan[2] have been used to arrive at the convective heating rates, whereas the radiative heating rates have been obtained from available thermal and plume analysis methods. A jet plume method-of-characteristics program[3] was used to determine the gaseous plume characteristics of the SRM's.

Full Base Close-Out Heat Shield

As shown in Fig. 1, no jet impingement is experienced during the SRM operation in the first 70 sec; therefore, the convective base recirculation segment of the total heat transfer is negligible. However, radiation from the aluminum oxide particles is significant. Thus, the predominant heating mode considered during the initial phase of boost is radiation heat transfer. The solid-particle plume may be approximated geometrically by a circular cone frustum[4] with a half-angle identical to that of the engine nozzle half-angle. Each plume is arbitrarily truncated by a plane perpendicular to the nozzle axis at a centerline length of 50 ft. The solid-particle plume radiates as a blackbody,[5] and the emitted radiation heat flux from flight data has been found to vary from 35 to 50 Btu/sec-ft^2 of plume area.[4] These values are considered constant and independent of altitude. Heat transfer to various locations in the base area is computed by utilization of the view factors provided by the CONFAC[6] program. The planar-conical surface of the SRM conical frustum is generated automatically as an option by this program.[6] The radiation heat-transfer results obtained by this analysis are shown in Fig. 2. The peak heating rate does not occur over the center element but rather reaches a maximum at the element adjacent to the geometric center on the diagonal rays.

Inner Heat Shield

After ejection of the full base close-out and ignition of the J-2 engines, the plume characteristics of the SRM (again using Ref. 3) and J-2 engines must be determined to predict the onset of full base recirculation and resultant choking of the flow in the base. Available data[7] for the J-2 engine provided the plume boundaries at identical altitudes and until J-2 burnout. These boundaries were utilized to arrive at a composite plume picture during J-2/SRM operation and further until J-2 burnout (Fig. 1). The point on the inner heat shield chosen for analysis is directly between the J-2 engines slightly inboard of the pitch circle diameter, where experimental convective heating data[8] for the present S-II configuration (Fig. 3) indicate a maximum for fully choked flow. The location of maximum radiative heating approximately coincides with the point of maximum convective heating exclusive of the shielding effect of the nozzles. The solid-particle radiation calculations are made as previously outlined except that the J-2 nozzles shield the elemental area from the majority of diametrically oriented SRM plumes; i.e., the radiant heat input will be twice that from one of the two nearer SRM plumes. Therefore, the incident radiative heat flux for the selected point on the S-II inner heat shield is 12.5 Btu/ft^2-sec.

Present S-II convective heating rates[8] have been obtained by experimental means and are considered valid for fully choked flow that exists in a high-vacuum environment for the base geometry of the S-II configuration. However, for this study with ignition at 30,000 ft, the base flow is still in the aspiratory regime. Between 30,000 and 60,000 ft, jet impingement begins along with the associated base recirculation (Fig. 1). To establish the altitude and time at which the base flow becomes choked, a flow model was adopted[2] which relates the region of jet impingement (with its associated shock system) to the base pressure and a critical pressure ratio. The flow model in effect provides for two regions of choked flow. The first region is determined by the point of impingement of adjacent plume boundaries; here Chapman's criteria,[9] plume characteristics, oblique shock relations, and the expressions of one-dimensional isentropic flow are used to establish the base pressure and choked flow conditions. The second region of choked flow lies in the area between adjacent outboard engines where expansion to ambient pressure occurs. It is evident that full base recirculation is not established until both areas are fully choked. Applying the criteria previously established results in initiation of choking at approximately 60,000 ft with full base recirculation being reached at approximately 90,000 ft, where the present distribution of convective heating over the existing S-II heat shield may be applied. The transition from aspiratory to fully choked flow thus evaluated was used to formu-

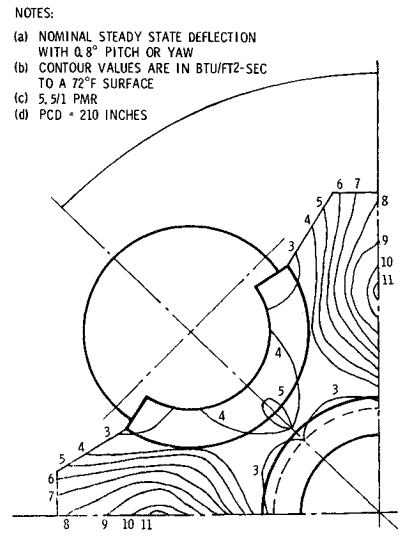

Fig. 3 Contours of design convective heat-transfer rate on S-II heat shield.

late the magnitude of convective heating rates during the transition period to full base recirculation.

The computer program described by Ostlund[10] was used to compute the convective heat transfer in the form

$$q_{\text{conv}} = h(i_r - i_w) \tag{1}$$

The value of h is not a strong function of surface temperature; hence the convective heat transfer is essentially a function of wall enthalpy only for a given recovery enthalpy. Therefore

$$q_{\text{conv}_2} = h(i_r - i_{w_2}) = q_{\text{conv}_1}(i_r - i_{w_2})/(i_r - i_{w_1}) \tag{2}$$

Substituting i_{w_1} evaluated at 72°F (532°R) and i_r evaluated at 3000°F (3460°R) (a temperature based upon experimental data), the result is

$$q_{\text{conv}_2} = q_{\text{conv}_1}(945 - i_{w_2})/820 \tag{3}$$

$$h = q_{\text{conv}_1}/820 \qquad (\text{lb/ft}^2\text{-sec}) \tag{4}$$

The radiation heat-transfer rate[8] from the H_2-O_2 combustion of the J-2 engines was assumed not to be affected by the nature of the base flow; e.g., these rates would apply during the entire operation of J-2 engine firing. Because of the magnitude of the radiation heat-transfer rates, i.e., on the order of 1 Btu/ft²-sec, in comparison to the convective and SRM radiation heat-transfer rates, this assumption has a relatively small influence on the total heat transfer.

The total heat transfer to the S-II inner heat shield was determined at the point of maximum convective heating (Fig. 3). The variation with time of the convective heating rate at the selected location was found by the previously described flow model and pressure criteria. To this was added the SRM radiation heat-transfer rate assuming superpositioning applies. The total heat-transfer rate variation with trajectory time for the S-II inner heat shield at the preselected point is shown in Fig. 4. During the period of combined SRM and J-2 operation, there is a peak in the heat-transfer rate to the S-II inner heat shield which lasts for approximately 25 sec, then the heating rate falls to the convective value after SRM burnout.

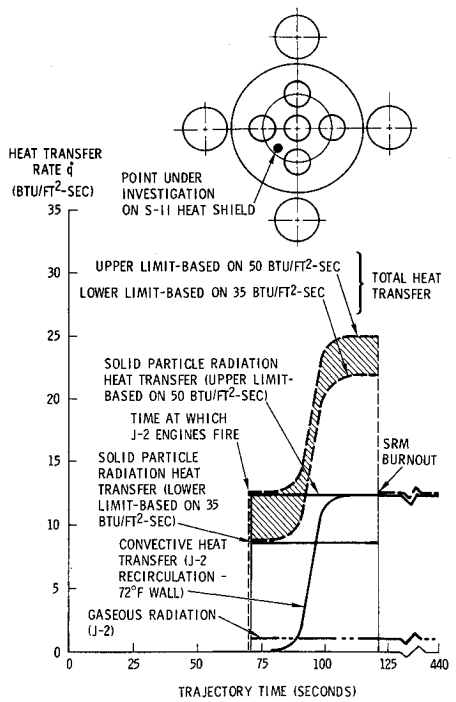

Fig. 4 Heat-transfer rate (convection, radiation, and total) vs trajectory time to selected point on S-II heat shield.

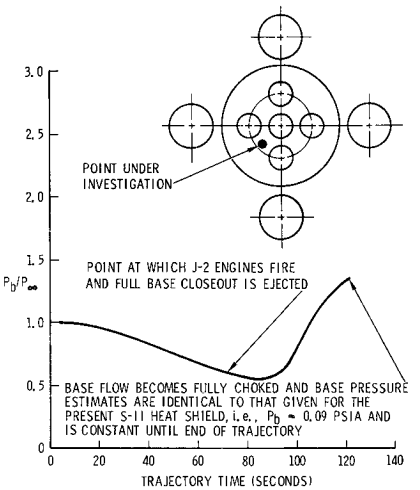

Fig. 5 Base pressure history of study vehicle.

Base Pressure Estimates

Because of the large pitch circle diameter of the SRM's it is assumed that the base pressure during the first 70 sec of boost can be determined by assuming no jet entrainment effects. Using Chapman's model,[9] which predicts the base pressure as a function of the vehicle's shoulder conditions, it is possible to establish the base pressure as a function of time up to the point of full base close-out ejection. To show the variation of base pressure from aspiratory to fully choked flow, a point on the base coinciding with the maximum convective heat transfer was selected. Applying the criteria previously established to predict base pressure during the aspirating phase, in addition to values through the transition stage, the base pressure variation with time at the preselected point was computed (Fig. 5).

Base Thermal Protection

The development of base thermal protection systems has had almost a decade of background for selection of suitable materials to meet the environments. Among the first materials considered suitable were the ablative types such as silicones, modified epoxy resins, and reinforced phenolic resins. The desire was to achieve low density and low thermal diffusivity while retaining a suitable char formation and a reasonable heat of ablation even in the presence of heat fluxes lower than the ballistic re-entry levels. Thus, the interest in castable and molded microballoon and cork-filled resin systems was initiated. For typical base heat fluxes and the low oxidizing environment of the current study, a molded cork board (AC-2755) impregnated with a modified phenolic resin has been selected for the purpose of comparing ablative system performance with a heat-resistant system.

Simultaneously, there has been much interest in the development of nonablative insulations for high-temperature applications, such as the leading edges of hypersonic aircraft. For the present application, the possibility of applying a low-density, highly reflective ceramic material was of special interest. The heavier materials such as alumina, zirconia, and graphite were eliminated on a weight basis, but the available low-density, foamed ceramics and colloidal silica suspensions warranted consideration.

The base-area thermal protection design must provide for isolation of critical base-area equipment and structure from the external heating identified in the thermal environment section. Although use of a single heat shield was suggested during the earlier studies, a two-heat-shield concept was chosen after the requirements for J-2 engine prestart conditioning had been investigated more thoroughly. In this concept, the first heat shield (full base close-out) maintains

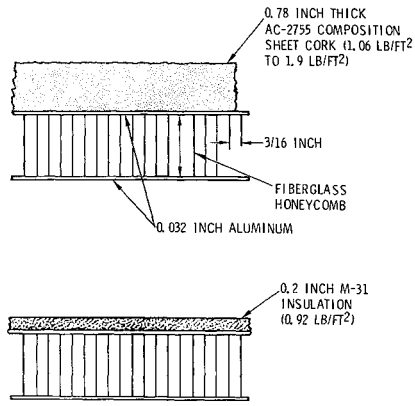

Fig. 6 Full base close-out thermal protection.

environmental protection for the J-2 engine preconditioning system during the first 70 sec of boost. The second or inner base heat shield protects base-area equipment when the base close-out shield is jettisoned at J-2 engine start-up. After the SRM's have been jettisoned (at 120 sec) the remaining thermal protection provided is essentially that of the present S-II base heat shield design. The required modification to the present design includes such items as radiation shields around the edges to avoid exposure of structure and equipment to the high heat sources.

This study provides analyses of both an ablative cork material and a nonablative ceramic material as the primary thermal protection elements and so offers an analytical basis for the optimum design selection for both the base close-out and inner base heat shields.

Full Base Close-Out Heat Shield

AC-2755 composition sheet cork (ablation design)

The material used in the ablative analysis is AC-2755 composition sheet cork,[11] which consists of finely ground cork particles held together with a phenolic resin, and is the same as that used for Minuteman thermal protection.[12] For relatively high heat inputs the material chars and rises quickly to a maximum radiating temperature of approximately 1200°F, relieving the heat load by reradiation on the order of 3 Btu/ft²-sec. The full base close-out heat shield (Fig. 6) consists of a backface sandwich structure of fiberglass honeycomb ($\frac{3}{16}$ GF-11-4.0) with 0.032-in.-thick aluminum facings, in addition to the external protection. The charring ablation model used in this analysis is adapted from Ref. 12. Since cork is a charring material, its density and thermal conductivity decrease as temperature increases and decomposition of the virgin cork occurs (selected variations are shown in Fig. 7). The cork material is bonded to the fiberglass honeycomb by an epoxy-phenolic adhesive, which fails at approximately 560°F. The additional cork properties[12] adopted are $C = 0.45$ Btu/lbm-°R, $\epsilon = 0.9$, and $\alpha = 1.0$. The property that may markedly fluctuate is the "heat of ablation," which is defined as the ratio of the gross heat input into the cork to the pounds of char removed under steady-state ablation. Note that this definition is based upon the density of the char, and not the virgin material for which most other ablation material data are given.

The high radiation-emitting temperature of the char loses its effectiveness in an enclosed environment where heat radiated will in turn be absorbed and reradiated back to the surface. The escaping gases from the reacting layer provide an effective means of blocking and/or shielding heat inputs. In a silo environment such as in the Minuteman application,[12] the associated higher pressures and relatively stagnant conditions result in mass blocking being more effective than in flight, where the gases are removed more quickly due to lower pressures and convective currents. These effects can cause the heat of ablation to vary between 5000 Btu/lbm for silo heating to 2500 Btu/lbm in a flight environment.[12]

When the virgin cork is decomposing, the heat input contributing to the sensible temperature rise must be examined on a unit volume basis. The total heat going into the sensible temperature rise within the slab can be expressed as

$$q^* = \left(\int_{T_1}^{T_2} C\rho dT\right) \Big/ \rho_{\text{char}}$$

Based upon the cork specific heat, $\rho(T)$ variation from Fig. 7, $T_1 = T_0 = 560$°R (an arbitrary initial temperature), and $T_2 = 1660$°R (the ablation temperature), the sensible heat rise that should be subtracted from the heat of ablation is 893 Btu/lbm$_{\text{char}}$. The assumption of a constant 2500-Btu/lbm$_{\text{char}}$ heat of ablation is reasonable in view of the small effect of initial temperature on the total heat of ablation and the previously mentioned fluctuation of the mass blocking effect. For example, an initial temperature change of 209°F is required to change a 2500-Btu/lbm heat of ablation by 10%. Further, the computer program[10] used for this calculation was originally intended for subliming ablators and was modified to take into account the density variation when computing the sensible heat rise of an element. Thus, initial temperature differences of elements are neglected and the flight environment for the base region determines the effect of mass blocking.

The ablation program[10] was utilized to compute the ablation of the center element on the full base close-out heat shield, which is subjected to a constant radiation heat input of 25.1 Btu/ft²-sec for a duration of 70 sec. Since an absorptivity of 1 was assumed, none of the impinging radiation is reflected. Initially, the criterion for determining the thickness of the cork was to keep the backface temperature below 560°R (since this would still allow the J-2 engines to remain precooled—a condition necessary to insure proper ignition), assuming an initial inside surface temperature of 360°R, and ambient temperature on the outside face. However, after examination of the results of the preliminary computer runs, it was seen that the high heat input and accompanying rapid movement of the ablating (charring) interface creates such high surface temperature gradients that virtually all of the cork must be charred before any heat reaches the backface.

This may be seen by examining the problem of a semi-infinite slab ablating at the plane $x = 0$, where the slab in the region $x > 0$ moves toward this plane with speed, $-U$. The one-dimensional differential equation governing this problem[13] is

$$\frac{\partial V}{\partial t} - U\frac{\partial V}{\partial x} - \frac{k}{\rho C}\frac{\partial^2 V}{\partial x^2} = 0 \qquad (5)$$

where $V(x,t) = T(x,t) - T_0(\infty,t)$; $T(0,t) = 1660$°R; and $T_0(\infty,t) = 360$°R. The solution to Eq. (5) satisfying the boundary conditions is

$$T(x,t) - T_0(\infty,t) = [T(0,t) - T_0(\infty,t)]e^{-U\rho Cx/k} \qquad (6)$$

Now if $T(x,t) = 560$°R, i.e., the backface temperature requirement, and

$$U = q_{\text{NET}}/\rho H \qquad \text{where} \qquad q_{\text{NET}} = q_{\text{in}} - q_{\text{rad}} \qquad (7)$$

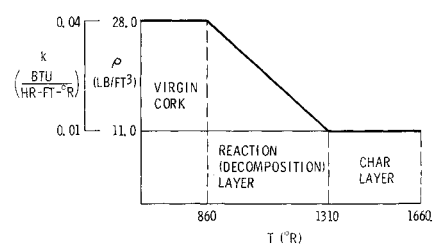

Fig. 7 Variation of ρ and k with temperature.

then the equation becomes

$$200 = 1300e^{-q_{NET}Cx/Hk} \quad (8)$$

Taking $k = 0.04$ Btu/hr-ft-°R, which is the maximum conductivity[7] to find the largest x value, and substituting for q_{NET}, H, and C, the temperature drops from 1660° to 560°R in a distance of 0.053 in., further justifying the approximation (about $\frac{3}{4}$ in. of cork is ablated in 70 sec). Thus, a reasonable thickness and tailoring model may be established by assuming that all heat input goes into reradiation, phase change, and mass blocking. The thickness (in.) may be conveniently calculated by

$$x = \left(12\int_0^t q_{NET}\,dt\right)\Big/H\rho_{char} = \frac{12q_{NET}t}{H\rho_{char}} \quad (9)$$

or, leaving q_{NET} as a variable for a tailoring model,

$$x = 0.0306\,q_{NET} \quad (10)$$

Resultant thicknesses are presented in Fig. 8 for the known heat inputs across the full base close-out. Based upon a virgin cork density of 28 lb/ft³, $W = 0.0714\,q_{NET}$ (lb/ft²) for the base close-out. For the center element heat input of 25.1 Btu/ft²-sec, the areal density is 1.78 lb/ft².

M-31 insulation material[14] *(nonablative)*

An alternate thermal protection scheme to AC-2755 Composition Sheet Cork is M-31, an inorganic, highly reflective material prepared from fibrous potassium titanate and asbestos fibers that are bonded with colloidal silica (Fig. 6). This coating was originally developed for protecting the base of the SATURN C-1 launch vehicle.[15] A protective coating of nitrocellulose is required to keep the outside surface from being contaminated during assembly and other handling operations and is rapidly consumed by the base heating without leaving any residue that would offset the optical properties of the M-31.

The mechanical and thermodynamic properties of M-31 must be averaged because of the anisotropy of the material and fluctuations through the thickness, which are primarily due to the troweling application and migration of silica particles to the surface during drying. This latter result is observable in a density gradient through the material which is characterized by a hard exterior and a soft interior; however, recent available data indicate that there is a procedure for gelling the colloidal silica to minimize migration of the particles. Ordinary M-31 density may vary from 82 lb/ft³ to 25 lb/ft³, and for this study an average density of 55 lb/ft³ was used. All property measurements are on M-31 without mechanical reinforcement that would be necessary for bonding purposes in practical application (the reinforcement is usually a honeycomb core).

The thermal conductivity in the direction normal to the plane of application increases from 0.071 Btu/hr-ft-°R at 560°R to 0.108 Btu/hr-ft-°R at 1190°R, and the conductivity is assumed to vary linearly above this range. Thermal

Table 1 Properties of S-II inner heat shield[a]

Material	t, in.	ρ, lb/ft³	k, Btu/hr-ft°R
Hot face (S-994 glass)	0.030	115	∞
Core-siloon	1.000	4	0.038 @ 260°R
			0.040 @ 860°R
			0.050 @ 1260°R
			0.180 @ 2460°R
Mid-face (S-994 glass)	0.046	115	∞
Core	1.000	2	0.020 @ 460°R
			0.520 @ 2460°R
Cold face (181 glass)	0.036	115	∞

[a] Specific heat of all materials is approximately 0.4 Btu/lbm°R.

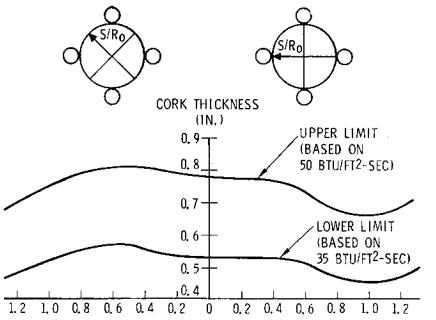

Fig. 8 Tailoring of full base close-out thermal protection.

properties used in the analysis of M-31 are $C = 0.31$ Btu/lbm°R, $\epsilon = 0.4$, and $\alpha = 0.2$. In 70 sec of radiant heat input, a 0.2-in. thickness of M-31 insulation material restricts the hot side of the backup structure to approximately 660°R and limits the exposed surface temperature to 1900°R. An average per unit area weight of 0.92 lb/ft² was then calculated for the M-31 insulation material by the thermal analysis program.[10]

It is clear from the foregoing analysis that the M-31 nonablative thermal protection has a distinct advantage over the ablative cork. The weight per unit area of these systems is 0.92 lb/ft² and 1.78 lb/ft², respectively, indicating that the M-31 insulation offers approximately an 800-lb savings over the total area of 900 ft².

Inner Heat Shield

The S-II inner heat shield (Fig. 9) consists of two honeycomb structures separated and faced by glass cloth. The upper core (hot side) is filled with siloons whereas the bottom core (cold side) has no fillers. Also, each bondline to a core has approximately 0.01 in. of adhesive. Thermal gradients across the faces and adhesive can be neglected because of the high conductivities of these materials. The empty honeycomb structure transmits heat by conduction through the core walls and by radiation between the faces, with an equivalent conductivity used to describe both processes. The properties of the structure are contained in Table 1. The present S-II heat shield can withstand the heat loads imposed upon the present S-II base region when the vehicle is used as a second stage, but when the SRM's are added, additional heat protection must be provided. Either the AC-2755 Composition Sheet Cork (charring ablation) material or the M-31 insulation may be bonded to the present heat shield. The bondline temperature must be kept below 960°R during the period when the SRM's are firing; after this period, the present heat shield is adequate. The nozzles projecting outward from the shield partially block emitted heat from the shield and are accounted for by assuming a configuration factor of 0.9, and result in an effective emittance of 0.9ϵ.

It was found that a 0.35-in. thickness of cork (weighing 0.82 lb/ft²) is sufficient to maintain an adequate bondline temperature until SRM burnout. At this time, approximately 0.32 in. of cork have ablated away leaving enough

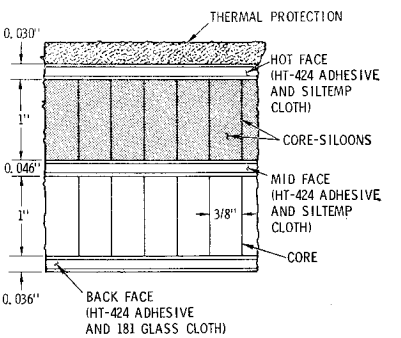

Fig. 9 S-II inner heat shield structure (not to scale).

material to insulate the shield face from the high temperatures near the ablation surface.

The M-31 insulation, which does not exhibit a phase change and therefore has a variable surface temperature, is more sensitive than cork to the rate of heat input. A 0.2-in. thickness is sufficient to keep the bondline temperature down to 960°R at a hot surface temperature of 2060°R at 120 sec. At this time (SRM burnout) the surface temperature starts to decrease, since the net heat absorbed by the surface has been lowered by 2.5 Btu/ft²-sec, and the hot surface emits 4 Btu/ft²-sec, which, combined with internal conduction, dissipates heat faster than the 6-Btu/ft²-sec convective heating rate. This transient phenomena lowers the outside surface temperature, but heat continues to be conducted into the protected shield surface until the thermal gradients "relax" enough to "support" the lessened heat impulse. Thus, the heat capacity of the M-31 contributes to raising the heat shield temperature. The emissivity of 0.4 for the M-31 is less conducive to rejecting the convective heat input and thus causes the surface temperature to stabilize at a higher level than the current S-II heat shield. Since a 0.2-in.-thick layer of M-31 insulation weighs 0.92 lb/ft², it does not compare favorably with cork protection, which 1) weighs 0.82 lb/ft² and 2) is easier to apply. Thus, cork is chosen for use on the inner heat shield.

Conclusion and Summary

During the first 70 sec of flight no jet impingement occurs between the SRM's, and the predominant mode of heat transfer to the full base close-out is from the solid-particle radiation. The incident radiation from the aluminum oxide particles varies from 26 to 22 Btu/ft²-sec at various locations on the full base close-out. Whereas approximately 0.75 in. (1.78 lb/ft²) of AC-2755 Composition Sheet Cork would be needed to protect the backup structure until the full base close-out is ejected, only 0.2 in. (0.92 lb/ft²) of a heat-resistant thermal protection material (M-31) would be needed. The 0.86-lb/ft² difference in weight implies about 800 lb lift-off weight savings for the heat-resistant M-31 design.

After full base close-out ejection, the radiation received by the inner heat shield is reduced to 12.5 Btu/ft²-sec at a point between the J-2 engines where maximum convective heating will be expected to occur after the onset of full base recirculation of the J-2 plumes. At 120 sec, the SRM's cease operation, having contributed no convective heat input. The J-2 plumes impinge at 40,000 ft (60 sec), and the convective heat input builds up from the initiation of full base recirculation at 60,000 ft (88 sec) until fully choked flow occurs at 90,000 ft (100 sec) when a maximum convective input of 12.5 Btu/ft²-sec is reached. The overlap of the SRM and J-2 operation creates a peak in the (cold base) total heat-transfer rate of 25 Btu/ft²-sec for approximately 25 sec, which reduces to the maximum convective value of 12.5 Btu/ft²-sec after SRM burnout. In this case, a 0.35-in. thickness (0.82 lb/ft²) of cork on the inner heat shield is adequate to keep the bondline temperature below 960°R until 120 sec (after which time the present S-II heat shield is adequate), whereas 0.2 in. (0.92 lb/ft²) of M-31 would be needed. Thus, use of cork on the inner heat shield should save 11% in weight, and cork would be easier to apply.

In conclusion, the superior reflective properties of the M-31 make it a suitable material for thermal protection against the predominantly radiative heat flux of the SRM plume. When the incident heating has a sizable convective component (J-2 engine operation) it is more important to secure the ablative heat absorption and high surface emittance provided by cork.

References

[1] Fraser, G. F., Denison, D. E., and Kaysen, H. M., "Studies of improved Saturn V vehicles and intermediate payload Saturn vehicles," North American Aviation, Inc., Space Div., SID 66-1326 (October 1966).

[2] Etemad, G. A. and Korkan, K. D., "Base flow characteristics and thermal environment of launch vehicles with strap-on solid rocket motors," *Proceedings of the American Astronautical Society Southeastern Symposium on Missiles and Aerospace Vehicle Sciences* (American Astronautical Society, Huntsville, Ala., 1966), pp. (14–1)–(14–14).

[3] Rashidian, R. M., "General description of the flow properties of a jet plume by method of characteristics (AP-214), Vol. II," North American Aviation, Inc., Space Div., SID 66-423 (August 1966).

[4] Kramer, O. G., "624A program solid rocket motor base heating environment," private communication, Aerospace Corporation, El Segundo, Calif. (February 1966).

[5] Morizumi, S. J. and Carpenter, H. J., "Thermal radiation from the exhaust plume of an aluminized composite propellant rocket," J. Spacecraft Rockets **1**, 501–507 (1964).

[6] Toups, K. A., "CONFAC II—A general computer program for the determination of radiant interchange configuration and form factors," North American Aviation, Inc., Space Div., SID 63-1397 (January 1964).

[7] Laspesa, F. S., private communication, S-II Vehicle Systems, North American Aviation, Inc., Space Div., Downey, Calif. (May 1966).

[8] Ali, A., "S-II environmental data for S-II stage," North American Aviation, Inc., Space Div., SID 61-473-1 (1965).

[9] Chapman, D. R., Keuhn, D. M., and Larson, H. K., "Investigation of separated flows in supersonic and subsonic streams with emphasis on the effect of transition," NACA Rept. 1356 (1958).

[10] Ostlund, R. A., "Calculation of transient temperatures in ablating and non-ablating bodies using a digital computer," North American Aviation, Inc., Columbus Div., NA 60H-460 (January 1961).

[11] Hovey, R. W., "Cork thermal protection design data for aerospace vehicle ascent flight," J. Spacecraft Rockets **2**, 300–304 (1965).

[12] Herold, L. M. and Diamant, E. S., "Thermal performance of cork insulation on Minuteman missiles," J. Spacecraft Rockets **3**, 679–684 (1966).

[13] Carslaw, H. S. and Jaeger, J. C., *Conduction of Heat in Solids* (Oxford University Press, New York, 1959), 2nd ed., p. 292.

[14] Seitzinger, V. F., "Further development and evaluation of M-31 insulation for radiant heating environments," NASA TM X-53267 (May 1965).

[15] Seitzinger, V. F., "Development of a highly reflective unfired ceramic thermal insulation," George C. Marshall Space Flight Center, MTP-P&VE-M-62-14 (December 1962).